# Collisional loss of cesium Rydberg atoms in a magneto-optical trap

Zhigang Feng, Hao Zhang, Junling Che, Linjie Zhang, Changyong Li, Jianming Zhao,* and Suotang Jia
*State Key Laboratory of Quantum Optics and Quantum Optics Devices, College of Physics and Electronics Engineering, Shanxi University, Taiyuan 030006, China*
(Received 21 December 2010; published 25 April 2011)

The collisional loss rates of $63S_{1/2}$ Rydberg atoms in cesium magneto-optical trap are measured by using the state-selective pulse field ionization technique and used to investigate the interaction between Rydberg atoms. The collisional loss rate coefficients due to collisions with Rydberg atoms and ground-state atoms are obtained by fitting the experimental data. The results indicate that the large collisional loss mainly comes from the strong long-range interaction between ultracold Rydberg atoms, and the loss rate is significantly increased under a weak electric field.

DOI: 10.1103/PhysRevA.83.042711 PACS number(s): 34.90.+q, 32.80.Ee, 37.10.De

## I. INTRODUCTION

In recent decades, the collisions of Rydberg atoms have been extensively studied both experimentally and theoretically due to their large size and low binding energy [1], which play an important role in the atomic and molecular physics and many laser applications. Due to the limitations of the large thermal velocities, many atomic beam experiments have mainly focused on the relevant low-lying Rydberg states [2].

Recently, the collision properties at ultralow temperatures have opened new research areas in atomic, molecular physics, and chemical physics with the help of laser cooling and trapping techniques. In contrast to thermal atomic experiments, collisions between cold atoms offer many interesting features connected with their low collision energy and long collision duration. Collisions become very sensitive to long-range interactions and to the absorption and emission of radiation during the collision time [3], e.g., collision loss in single-species [4] or two-species [5] magneto-optical-trap systems, and atom-molecule and molecule-molecule collisions [6]. In additional, the ultracold Rydberg atoms have been extensively investigated in many-body collisions [7,8], state mixing [9,10], lifetime measurements [11], and spontaneous evolution into ultracold plasmas [12]. Due to their large cross sections and polarizabilities, ultracold Rydberg atoms exhibit strong, tunable resonant dipole-dipole or off-resonant van der Waals interactions. One fascinating effect is the interaction-induced blockade effect [13,14], which has been proposed as a crucial ingredient for quantum-information processing [15]. The strong interactions also lead to extreme collisional properties of ultracold Rydberg atoms. The longer interaction time and narrower velocity distribution of ultracold Rydberg atoms allow for observation of the collisional processes and dynamic evolution in more detail. A weak background dc electric field can change the potential curve dominating the collision process of Rydberg atoms [16], and even forming Rydberg molecules by modifying the avoided crossings between Rydberg atom-pair interaction potentials [17]. The electric field also can be used to tune the interaction between Rydberg dipole-allowed states, and even cause the excitation of dipole-forbidden but quadrupole-allowed transitions, which open additional transition channels and have been investigated in ultracold Rb Rydberg atoms [18]. Therefore, understanding and controlling the collisional properties between Rydberg atoms provides an excellent platform for the study of Rydberg atomic interaction and Rydberg atom-pair excitation processes. However, most works on Rydberg atomic interactions were focused on the principal quantum number $n < 50$ [19–21]. For higher $n$, Rydberg atoms exhibit strong long-range interaction, which has a dramatic effect on the excitation dynamic. For example, suppression of excitation corresponding to the van der Waals interactions had been studied in excitation of high Rydberg states ($n \sim 70$–$80$) using a pulsed amplified single-mode laser [13]. In additional, the strong-interaction-induced collision can also give rise to the rapid decay of Rydberg atoms and even energy transfer [19]. The decay of Rydberg atoms is one of the effects induced by the interaction between Rydberg atoms. We measured the decay rate of a high Rydberg state and obtained interaction information (including long-range interaction and dipole interaction induced by an electric field applied at the same time).

In this paper, we investigate the collisional loss of $63S_{1/2}$ Rydberg atoms in a cesium magneto-optical trap (MOT) using the state-selective pulse field ionization technique. We extract the collisional loss rate coefficients between Rydberg atoms by measuring the temporal behavior of Rydberg atomic population at zero electric field and a weak applied electric field. We also obtain the collisional loss rate coefficient due to collisions with the ground-state atoms.

## II. EXPERIMENTAL SETUP

We cool and trap cesium atoms in a standard MOT at a temperature of $\sim$100 $\mu$K. The trap has a Gaussian radius of 400 $\mu$m and contains $\sim 6\times10^7$ cold atoms, which lead to a peak density on the order of $10^{11}$ cm$^{-3}$. The experimental setup is shown schematically in Fig. 1. Excitation to Rydberg states is accomplished by a two-photon scheme; the first photon is provided by the cooling and trapping laser (Toptica, DL100) with a wavelength of 852 nm. The second photon is generated by a commercial laser system (Toptica, TA-SHG110) consisting of an extended cavity diode laser which is amplified to a maximum power of 1 W and then doubled to 507–517 nm with a linewidth below 2 MHz. The output beam of the 510-nm laser is switched on for typically1 $\mu$s

*zhaojm@sxu.edu.cn

 

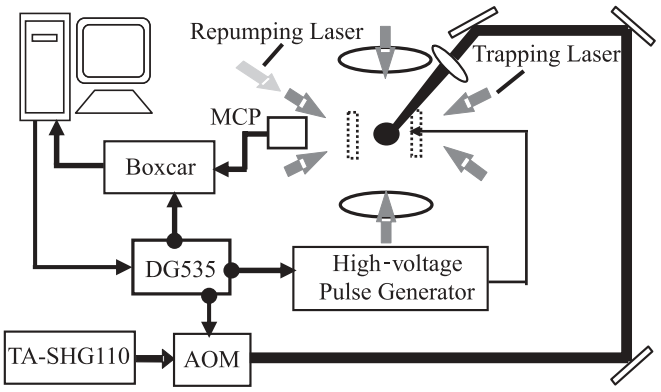


FIG. 1. Experimental setup. MCP: microchannel plate, AOM: acousto-optical modulator.

with an acousto-optical modulator (AOM), and focused into the cold atomic cloud with a maximum power of 60 mW and a waist radius $\sigma_{\mathrm{Ry}} \sim 150\ \mu$m. The excited Rydberg atoms are located at the center of two parallel metal grids spaced 15 mm apart with an optical transmission of 95% through which the MOT laser beams pass almost undisturbed. We apply a static voltage to one of the grids during the whole experiment, which allows us to compensate for the residual electric field and investigate the effect of an applied dc electric field $\varepsilon$ on interaction between Rydberg atoms. To the other grid we apply a 3-$\mu$s rise-time high-voltage electric-field pulse $[E = 1/(16n^4)]$ to ionize Rydberg atoms, and drive the ions to a microchannel plate detector (MCP) located behind one of the girds. A boxcar integrator is set to select the desired time-of-flight window, and the resulting data of averaging over five measurements are stored in a computer. The number of Rydberg atoms is obtained using a calibrated digital charge-coupled device (CCD) camera (IMC-82FT, IMT Tech.) by measuring the decrease in fluorescence of $6P_{3/2}$ atoms, which is consistent with the number of detected ions by a calibrated MCP with a quantum detection efficiency of 45%. The density of Rydberg atoms can be calculated by dividing the number of Rydberg atoms by an effective excitation volume $V_{\mathrm{exc}} = (2\pi\sigma_{\mathrm{Ry}}^2)^{3/2}$, with a typical peak density of $nS_{1/2} \sim 9 \times 10^9\ \mathrm{cm}^{-3}$.

While the Rydberg atoms are produced, the Rydberg atomic population can evolve freely during the delay time between the 510-nm laser pulse and high-voltage pulse field, which is controlled by a digital delay and pulse generator (SRS-DG535). The decay curve based on the high-resolution spectroscopy of $nS_{1/2}$ states is obtained by scanning the frequency of the 510-nm laser for different delay times at fixed initial Rydberg atomic densities. The absolute laser frequency is recorded using a commercial wavelength meter (HighFinesse-Angstrom, WSU-30) with an accuracy of 0.001 $\mathrm{cm}^{-1}$.

## III. RESULTS AND DISCUSSION

The collisional loss rate is determined from the analysis of the decay curve. The decay of the number of ultracold Rydberg atoms as a function of delay time is given by the following rate equation:

$$\frac{dN_{\mathrm{Ry}}}{dt} = -\alpha N_{\mathrm{Ry}} - \beta \int_V n_{\mathrm{Ry}}^2\, d^3r - \beta_{\mathrm{Ry}-G} \int_V n_{\mathrm{Ry}} n_G\, d^3r, \tag{1}$$

where $\beta$ is the loss rate coefficient caused by collisions between ultracold Rydberg atoms, $\beta_{\mathrm{Ry}-G}$ is the loss rate coefficient caused by collisions between ultracold Rydberg and trapped ground-state atoms, $n_{\mathrm{Ry}}$ and $n_G$ are the densities of Rydberg and ground -state atoms, respectively, and $\alpha$ is the loss rate coefficient mainly caused by the spontaneous radiation and blackbody radiation. Here, we neglect hot background gas collisions (composed mostly of hot Rydberg and ground-state atoms) due to the relatively low density of hot ground-state atoms in our experiment; while the hot Rydberg atoms are mostly removed by tuning the trapping laser into resonance before the arrival of the 510-nm laser pulse.

The integration in Eq. (1) is performed over the whole volume occupied by the excited Rydberg atoms. The spatial distribution for both ultracold Rydberg and ground-state atoms is approximately described by a Gaussian distribution [22], $n_{\mathrm{Ry}}(r,t) = n_0^{\mathrm{Ry}}(t)e^{-r^2/2\sigma_{\mathrm{Ry}}^2}$ and $n_G(r,t) = n_0^G(t)e^{-r^2/2\sigma_G^2}$; substituting $n_{\mathrm{Ry}}(r,t)$ and $n_G(r,t)$ into Eq. (1) and integrating over the volume we obtain

$$\frac{dN_{\mathrm{Ry}}}{dt} = -\alpha' N_{\mathrm{Ry}} - \frac{\beta}{\left(4\pi\sigma_{\mathrm{Ry}}^2\right)^{3/2}} N_{\mathrm{Ry}}^2, \tag{2}$$

where

$$\alpha' = \alpha + \beta_{\mathrm{Ry}-G} N_G \left[\frac{1}{2\pi\left(\sigma_{\mathrm{Ry}}^2 + \sigma_G^2\right)}\right]^{3/2}. \tag{3}$$

Integrating Eq. (2) with respect to time yields

$$N_{\mathrm{Ry}}(t) = \frac{\left(4\pi\sigma_{\mathrm{Ry}}^2\right)^{3/2}\alpha' N_{\mathrm{Ry}}(0)e^{-\alpha' t}}{\left(4\pi\sigma_{\mathrm{Ry}}^2\right)^{3/2}\alpha' + \beta N_{\mathrm{Ry}}(0) - \beta N_{\mathrm{Ry}}(0)e^{-\alpha' t}}, \tag{4}$$

where $N_{\mathrm{Ry}}(0)$ is the number of initial Rydberg atoms. The experimental procedure to measure $\beta$ and $\beta_{\mathrm{Ry}-G}$ are carried out as follows: First, we compensate the residual electric-field components perpendicular to one of the grids by applying a small voltage of ~600 mV; the decay curve of the Rydberg atomic population is then measured by changing the delay time at a fixed initial Rydberg atomic density. Finally, we obtain the rate coefficients $\alpha\prime$ and $\beta$ by fitting the decay curve using Eq. (4). In order to extract the value of $\beta_{\mathrm{Ry}-G}$, we are required to estimate the value of $\alpha$, $\sigma_{\mathrm{Ry}}$, and $\sigma_G$. The $\sigma_G$ is derived from the CCD images of the cold atomic sample, while the $\sigma_{\mathrm{Ry}}$ is determined by measuring the waist of the excitation laser beam at the focus using the scanning knife-edge beam profile measurement technique. The values of spontaneous radiation rate and blackbody radiation rate come from theoretical calculations. Recently, Beterov *et al.* [23] have numerically calculated the zero-Kelvin lifetimes and blackbody-radiation-induced depopulation rate for higher Rydberg states $n \leqslant 80$ at several ambient temperatures by using the quasiclassical approximation method. A simple analytical

TABLE I. Value of the coefficients $A$, $B$, $C$, and $D$ in Eq. (6) for Cs [23].

| State | $A$ | $B$ | $C$ | $D$ |
|---|---|---|---|---|
| $nS_{1/2}$ | 0.123 | 0.231 | 2.517 | 4.375 |
| $nD_{3/2}$ | 0.038 | 0.076 | 1.790 | 3.656 |
| $nD_{5/2}$ | 0.036 | 0.073 | 1.770 | 3.636 |

expression for the zero-Kelvin spontaneous radiation rate can be written as

$$\Gamma_{\text{spon}} = \frac{1}{\tau_0} = \frac{1}{\tau_s n_{\text{eff}}^{\gamma}}, \tag{5}$$

where $\tau_s$ and $\gamma$ are fitting parameters determined by fitting the numerical results of zero-Kelvin radiative lifetimes as a function of effective principal quantum number $n_{\text{eff}} = n - \delta_l$, where $\delta_l$ is the quantum defect for a given state which is taken from Ref. [24].

The blackbody-radiation-induced depopulation rate can be approximately described by the following analytical function [23]:

$$\Gamma_{\text{BBR}} = \frac{A}{n_{\text{eff}}^{D}} \frac{2.14 \times 10^{10}}{\exp\left(315\,780 B / n_{\text{eff}}^{C} T\right) - 1} \ (\text{s}^{-1}), \tag{6}$$

where $T$ is the thermal background temperature; we assume that the vacuum chamber is 300 K for our experiment. The fitting parameters $A$, $B$, $C$, and $D$ were obtained from the fit of the numerical results at the temperature of 300 K and corresponding values for Cs are given in Table I.

Figure 2 shows a typical decay curve of $63S_{1/2}$ as a function of delay time at $\varepsilon = 0$ mV/cm and corresponding fitting curve. Each data is the result of Lorenzian fit to the $63S_{1/2}$ spectrum averaging over four individual scans, and normalized to a maximum signal at a 0 $\mu$s delay time. The ion spectrum of the $63S_{1/2}$ state at a delay time of 17 $\mu$s is shown in the inset of Fig. 2. We obtain the rate coefficients $\alpha' = (24\,480 \pm 480)\ \text{s}^{-1}$ and $\beta = (3.0 \pm 1.0) \times 10^{-6}\ \text{cm}^3/\text{s}$ by fitting the decay curve using Eq. (4). The error source mainly comes from the uncertainty in the measurement of the Rydberg atomic density. We can estimate $\alpha = 9302\ \text{s}^{-1}$ as the sum of the spontaneous radiation and blackbody radiation rates by Eqs. (5) and (6), and corresponding fitting coefficients are taken from Ref. [23]. We then extract the $\beta_{\text{Ry}-G} \sim (3.1 \pm 1.5) \times 10^{-7}\ \text{cm}^3/\text{s}$ from Eq. (3), which is one order of magnitude smaller than the collisional loss rate coefficient $\beta$. It is proved that the collisional loss due to collisions between Rydberg atoms is the dominant loss mechanism because of their strong interaction. Although the interaction potential is repulsive for $63S_{1/2}$ [25], the blackbody radiation can cause redistribution to an energetically nearby dipole-coupled Rydberg state, and give rise to collisional ionization. We experimentally observe that ions appear after a 10 $\mu$s delay time and increase with increasing delay time, and similar behaviors have been observed in Ref. [26] for higher Rb Rydberg states.

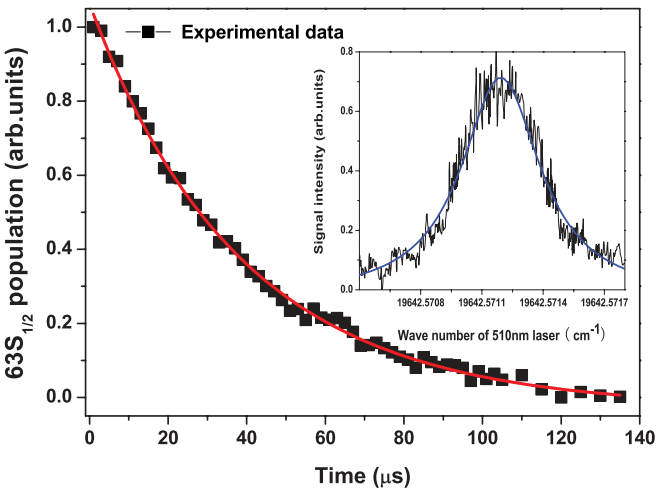


FIG. 2. (Color online) Typical decay curve of the $63S_{1/2}$ population as a function of delay time at a dc electric field of $\varepsilon = 0$ mV/cm. The red solid line represents a fitting of Eq. (4) to the data. The inset is spectrum of the $63S_{1/2}$ Rydberg state and Lorenzian fitting curve at a delay time of 17 $\mu$s.

Recent results indicate that a weak electric field can significantly change the potential curves of field-free Rydberg atoms pair, which lead to Rydberg atomic population transfer from an initial state to higher-$n$ states by some energy crossings, and eventual Penning ionization [16]. We also observe a similar effect in our experiment. Figure 3 shows the dependence of the $63S_{1/2}$ atomic population on a dc electric field at a fixed delay time of 3 $\mu$s. Obviously, the atomic population rapidly reduces with an increase of the dc electric field. In order to investigate the effect of the electric field on the interaction and further on the collisional loss rate, we measure the population of the Rydberg state as a function of delay time at a weak dc electric field and keep all other parameters fixed. The decay curve of $63S_{1/2}$ and the corresponding fit at $\varepsilon = 267$ mV/cm are shown in Fig. 4. Comparing to the experimental results at $\varepsilon = 0$ mV/cm, the presence of the electric field significantly accelerates the population decay from the initial Rydberg state. Because we keep all other experimental conditions unchanged except for the application of a weak electric field, we consider that the collisional loss rate between ultracold Rydberg and ground atoms is approximately

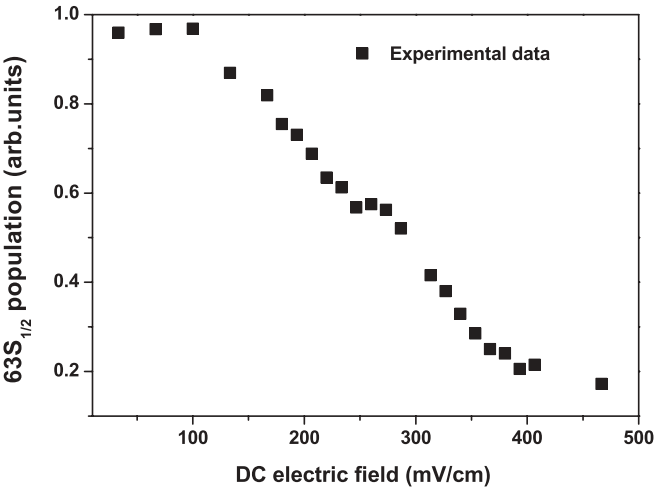


FIG. 3. The variation of the $63S_{1/2}$ atomic population with the dc electric field at a delay time of 3 $\mu$s.

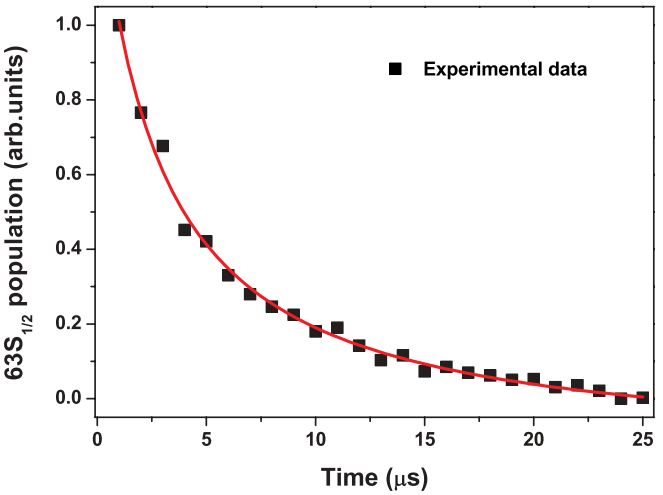


FIG. 4. (Color online) Typical decay curve of the $63S_{1/2}$ population as a function of delay time at a dc electric field of $\varepsilon = 267$ mV/cm. The red solid line is a fitting curve of Eq. (4) to the data.

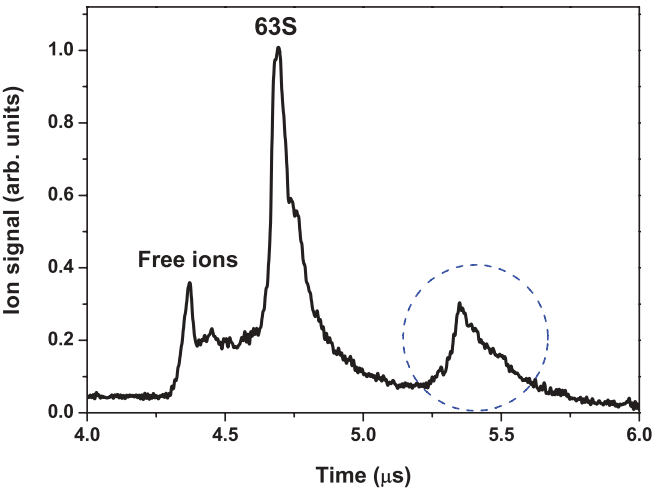


FIG. 5. Time-resolved ion signal of $63S_{1/2}$ with a dc electric field of $\varepsilon = 267$ mV/cm and fixed delay time of 6 $\mu$s. The data are normalized to its maximum signal. The signal enclosed in the circle represents dipole-allowed states induced by electric field.

constant. We therefore fix $\alpha\prime$ to a value from Fig. 2 and obtain a collisional loss rate coefficient $\beta = (3.7 \pm 1.4)\times 10^{-4}$ cm$^3$/s, which is two orders of magnitude larger than that of zero electric field. The large collisional loss rate is explained by the fact that the electric field can increase the interaction strength between the initial Rydberg state and the nearby dipole coupled states and transfer some Rydberg atoms to nearby states; the electric-field-induced dipole interaction (scaling as $R^{-3}$) is stronger than the long-range van der Waals interaction in the absence of an electric field (scaling as $R^{-6}$) at the same conditions.

It should be pointed out that the ion production is experimentally observed on slightly smaller time scales and rapidly increases with delay time as compared to the zero electric field. It confirms that the dc electric field increases the collisional possibility of Rydberg atoms and leads to increased collisional ionization, which maybe tune the interaction strength between coupled pair states by the electric field, because we observe the appearance of some dipole-allowed Rydberg states in a large electric field. Figure 5 shows the time-resolved ion signal for $63S_{1/2}$ at a dc electric field of $\varepsilon = 267$ mV/cm and a fixed delay time of 6 $\mu$s. A possible explanation is that the electric field induces nonadiabatic transition by forming energy crossings,and the influence of the dc Stark effect on the nonadiabatic multichannel decay of quasimolecules has been investigated [27]. The other possible reason is that pairs of $63S_{1/2}$ states are energetically degenerate with closer attractive pairs states for certain electric fields, and the electric field leads to $l$ and $n$ mixing between dipole-dipole coupled states. We will further investigate this process in other experiments.

## IV. CONCLUSION

We measure the collisional loss rate coefficients of cesium $63S_{1/2}$ Rydberg atoms at different background dc electric fields by measuring the corresponding decay curves in a conventional MOT. The large collisional loss of Rydberg atoms is mainly attributed to the collisions between ultracold Rydberg atoms because of their strong long-range interactions, which are one order of magnitude larger than the loss rate coefficients caused by collisions between ultracold Rydberg and trapped ground-state atoms. A weak dc electric field can significantly increase the collision loss by tuning the interaction strength between the coupled pair states. In fact, the Stark structures of the $nS$ states are mixed with the other states in the Stark manifold at an even weaker electric field for higher $n$ Rydberg states, which can result in many other effects such as energy transfer [14], dipole-forbidden transitions [18], and may even form Rydberg molecules. So the measurement of the collisional loss rate coefficient provides a tool for investigating the pair state dynamics in the electric field and interactions between Rydberg atoms.

## ACKNOWLEDGMENTS

The authors gratefully acknowledge useful discussions with J. H. Gurian. This work was supported by the NSFC Project for Excellent Research Team (Grant No. 60821004), and the National Natural Science Foundation of China (Grants No. 10934004, No. 60978018, and No. 61078001).

[1] T. F. Gallagher, *Rydberg Atoms* (Cambridge University Press, Cambridge, UK, 1994).

[2] K. A. Safinya, J. F. Delpech, F. Gounand, W. Sandner, and T. F. Gallagher, Phys. Rev. Lett. **47**, 405 (1981); D. S. Thomson, M. J. Renn, and T. F. Gallagher, *ibid.* **65**, 3273 (1990).

[3] J. Weiner, V. S. Bagnato, S. Zilio, and P. S. Julienne, Rev. Mod. Phys. **71**, 1 (1999).

[4] T. Walker and P. Feng, Adv. At. Mol. Opt. Phys. **34**, 125 (1994); J. Weiner, *ibid.* **35**, 45 (1995).
[5] L. J. Byron, R. G. Dall, and A. G. Truscott, Phys. Rev. A **81**, 013405 (2010).
[6] N. Zahzam, T. Vogt, M. Mudrich, D. Comparat, and P. Pillet, Phys. Rev. Lett. **96**, 023202 (2006); N. Syassen, T. Volz, S. Teichmann, S. Dürr, and G. Rempe, Phys. Rev. A **74**, 062706 (2006).
[7] W. R. Anderson, J. R. Veale, and T. F. Gallagher, Phys. Rev. Lett. **80**, 249 (1998).
[8] I. Mourachko, D. Comparat, F. de Tomasi, A. Fioretti, P. Nosbaum, V. M. Akulin, and P. Pillet, Phys. Rev. Lett. **80**, 253 (1998).
[9] A. Walz-Flannigan, J. R. Guest, J.-H. Choi, and G. Raithel, Phys. Rev. A **69**, 063405 (2004).
[10] W. Li *et al.*, Phys. Rev. A **70**, 042713 (2004).
[11] Z. G. Feng, L. J. Zhang, J. M. Zhao, C. Y. Li, and S. T. Jia, J. Phys. B **42**, 145303 (2009).
[12] M. P. Robinson, B. Laburthe Tolra, M. W. Noel, T. F. Gallagher, and P. Pillet, Phys. Rev. Lett. **85**, 4466 (2000).
[13] D. Tong, S. M. Farooqi, J. Stanojevic, S. Krishnan, Y. P. Zhang, R. Côté, E. E. Eyler, and P. L. Gould, Phys. Rev. Lett. **93**, 063001 (2004); K. Singer, M. Reetz-Lamour, T. Amthor, L. G. Marcassa, and M. Weidemüller, *ibid.* **93**, 163001 (2004).
[14] T. Vogt, M. Viteau, J. M. Zhao, A. Chotia, D. Comparat, and P. Pillet, Phys. Rev. Lett. **97**, 083003 (2006); T. Vogt, M. Viteau, A. Chotia, J. M. Zhao, D. Comparat, and P. Pillet, *ibid.* **99**, 073002 (2007).
[15] D. Jaksch, J. I. Cirac, P. Zoller, S. L. Rolston, R. Côté, and M. D. Lukin, Phys. Rev. Lett. **85**, 2208 (2000); L. Isenhower, E. Urban, X. L. Zhang, A. T. Gill, T. Henage, T. A. Johnson, T. G. Walker, and M. Saffman, *ibid.* **104**, 010503 (2010).
[16] A. Schwettmann, J. Crawford, K. R. Overstreet, and J. P. Shaffer, Phys. Rev. A **74**, 020701(R) (2006).
[17] K. R. Overstreet, A. Schwettmann, J. Tallant, D. Booth, and J. P. Shaffer, Nat. Phys. **5**, 581 (2009); S. M. Farooqi *et al.*, Phys. Rev. Lett. **91**, 183002 (2003).
[18] D. Tong, S. M. Farooqi, E. G. M. van Kempen, Z. Pavlovic, J. Stanojevic, R. Côté, E. E. Eyler, and P. L. Gould, Phys. Rev. A **79**, 052509 (2009).
[19] P. J. Tanner, J. Han, E. S. Shuman, and T. F. Gallagher, Phys. Rev. Lett. **100**, 043002 (2008).
[20] A. Reinhard, T. Cubel Liebisch, K. C. Younge, P. R. Berman, and G. Raithel, Phys. Rev. Lett. **100**, 123007 (2008); A. Reinhard, K. C. Younge, T. Cubel Liebisch, B. Knuffman, P. R. Berman, and G. Raithel, *ibid.* **100**, 233201 (2008).
[21] C. S. E. van Ditzhuijzen, A. F. Koenderink, J. V. Hernández, F. Robicheaux, L. D. Noordam, and H. B. van Linden van den Heuvell, Phys. Rev. Lett. **100**, 243201 (2008).
[22] F. P. D. Santos, F. Perales, J. Léonard, A. Sinatra, J. Wang, F. S. Pavone, E. Rasel, C. Unnikrishnan, and M. Leduc, Eur. Phys. J. D **14**, 15 (2001).
[23] I. I. Beterov, I. I. Ryabtsev, D. B. Tretyakov, and V. M. Entin, Phys. Rev. A **79**, 052504 (2009).
[24] K. H. Weber and C. J. Sansonetti, Phys. Rev. A **35**, 4650 (1987).
[25] K. Singer, J. Stanojevic, M. Weidemüller, and R. Côté, J. Phys. B **38**, S295 (2005).
[26] T. Amthor, M. Reetz-Lamour, C. Giese, and M. Weidemüller, Phys. Rev. A **76**, 054702 (2007).
[27] J. S. Cabral, J. M. Kondo, L. F. Gonçalves, L. G. Marcassa, D. Booth, J. Tallant, and J. P. Shaffer, New. J. Phys. **12**, 093023 (2010).